

1 Stable isotopes contain substantial additive information about terrestrial
2 carbon and water cycling.

3
4 Bonan Li^{a,b,c,d} Stephen P. Good^{a,b}, Richard P. Fiorella^{e,f,g}, Catherine E. Finkenbiner^{a,b},
5 Gabriel J. Bowen^{e,f}, David C. Noone^h, Christopher J. Stillⁱ, William R.L. Anderegg^{f,j,h}

6 ^aDepartment of Biological & Ecological Engineering, Oregon State University

7 ^bWater Resources Graduate Program, Oregon State University

8 ^cCollege of Earth Ocean and Atmospheric Sciences, Oregon State University

9 ^dDepartment of Biological & Agricultural Engineering, University of Arkansas

10 ^eDepartment of Geology and Geophysics, University of Utah

11 ^fGlobal Change and Sustainability Center, University of Utah

12 ^gEarth and Environmental Sciences Division, Los Alamos National Laboratory

13 ^hDepartment of Physics, University of Auckland

14 ⁱDepartment of Forest Ecosystems and Society, Oregon State University

15 ^jSchool of Biological Sciences, University of Utah

16 ^hWilkes Center for Climate Science and Policy, University of Utah

17 Corresponding author: Bonan Li

18 Email:libon@oregonstate.edu

Abstract

Stable isotope ratios of H (δ^2H), O ($\delta^{18}O$), and C ($\delta^{13}C$) are linked to key biogeochemical processes of the water and carbon cycles; however, the degree to which isotope-associated processes are reflected in macroscale ecosystem flux observations remains unquantified. Here through formal information assessment, new measurements of $\delta^{13}C$ of net ecosystem exchange (*NEE*) as well as δ^2H and $\delta^{18}O$ of latent heat (*LH*) fluxes across the United States National Ecological Observation Network (NEON) are used to determine conditions under which isotope measurements are informative of environmental exchanges. We find all three isotopic datasets individually contain comparable amounts of information about *NEE* and *LH* fluxes as wind speed observations. Such information from isotope measurements, however, is largely unique. Generally, $\delta^{13}C$ provides more information about *LH* as aridity increases or mean annual precipitation decreases. δ^2H provides more information about *LH* as temperatures or mean annual precipitation decreases, and also provides more information about *NEE* as temperatures decrease. Overall, we show that the stable isotope datasets collected by NEON contribute non-trivial amounts of new information about bulk environmental fluxes useful for interpreting biogeochemical and ecohydrological processes at landscape scales. However, the utility of this new information varies with environmental conditions at continental scales. This study provides an approach for quantifying the value adding non-traditional sensing approaches to environmental monitoring sites and the patterns identified here are expected to aid in modeling and data interpretation efforts focused on constraining carbon and water cycles' mechanisms.

Keywords: isotope, carbon flux, water flux, NEON, information theory

1. Introduction

Understanding the interactions and drivers of water and carbon exchanges between terrestrial ecosystems and the atmosphere is crucial to illuminate processes driving Earth's current climate as well as forecasting impacts of future change on ecosystems and the climate itself (Jung *et al* 2011, Piao *et al* 2020). To date, significant efforts have been made to monitor terrestrial carbon and water fluxes, including the widespread development of macroscale eddy covariance (EC) networks to measure ecosystem fluxes (Baldocchi 2014, Schimel and Schneider 2019). EC flux towers can measure continuous net ecosystem exchange (*NEE*) of CO₂ between the land surface and atmosphere at various frequency. Similarly, EC measurements of latent heat flux (*LH*), representing evaporation and transpiration from soils, water bodies, and plant canopies, provides valuable information for understanding regional and global water budgets as well as agricultural applications (Zhou *et al* 2018, Zeng *et al* 2020). Flux measurements have been used for a variety of environmental applications such as calibrating and validating remotely sensed flux estimations (Jia *et al* 2012), parameterizing land surface

models (Williams *et al* 2009), modeling seasonal crop coefficients (Li *et al* 2008), and investigating disturbance impacts such as post-fire carbon balance (Lupascu *et al* 2020). While measurements of LH and NEE can quantify fluxes themselves, new kinds of data are needed to refine knowledge of the processes driving these fluxes which are central to the carbon and water cycles.

To improve understanding of Earth system processes, the geoscience community has developed a wide array of advanced measurements to complement landscape scale flux data to help quantify environmental processes. These include studies focused on stable isotope fluxes (Dubbert and Werner 2019), Carbonyl Sulfide (COS) (Whelan *et al* 2018), various radiometric indices such as thermal (Still *et al* 2021) and solar induced fluorescence (SIF) (Guan *et al* 2016), and even environmental DNA (URycki *et al* 2022). Prominent among these techniques, naturally occurring water and carbon isotope measurements have been shown to be a powerful tool for understanding a wide array of ecohydrological and biophysical processes because distinct processes are, and are not, often associated with known isotope transformations (i.e., fractionation effects) (Bowen and Good 2015). Water isotope ratios (δ^2H and $\delta^{18}O$ in water) have been used to partition evapotranspiration into evaporation and transpiration, as evaporated and transpired fluxes from the same ecosystem may have distinct isotope ratios (Xiao *et al* 2018, Berkelhammer *et al* 2013). $\delta^{13}C$ values of CO_2 have also been applied to separate NEE into its constituent fluxes, as the isotopic composition of photosynthesis can differ from that of ecosystem respiration (Lee *et al* 2020). Previous network-based studies of δ^2H , $\delta^{18}O$ and $\delta^{13}C$ examined patterns across distinct ecosystems using cryogenic baths and flask samples; however, the poor temporal sampling and spatial coverage has limited these approaches to understand ecosystem-scale processes (Orlowski *et al* 2018, Gemery *et al* 1996). The development of automated laser spectroscopy systems mounted on EC towers provides new opportunities to obtain long term spatially and temporally resolved atmosphere profiles of these isotopes (Fiorella *et al* 2021). The recently launched National Ecological Observatory Network (NEON) provides the first standardized measurements of the stable isotope ratios of H_2O vapor and CO_2 for ecosystems across the USA that can be used to estimate δ^2H and $\delta^{18}O$ of LH and $\delta^{13}C$ of NEE (Finkenbiner *et al* 2022).

The development of advanced ecosystem measurements across networks such as NEON presents new scientific possibilities; yet this also raises the fundamental question of how useful new, and often expensive, data streams are for constraining uncertainties in targeted environmental processes. Many advanced measurements are made at considerable cost and effort, yet their full value as a source of information beyond traditional meteorological observations (e.g., vapor pressure deficit, VPD , air temperature, T , global radiation, R_g , and windspeed, u), is rarely demonstrated in a formal sense, especially within continental-scale networks where variability in environmental conditions occurs across a much wider range than individual sites. Here we capitalize on recent advances in information theory to assess the information content of NEON stable isotope data. These advances allow for the formal

quantification of linear and nonlinear interactions between variables (termed mutual information) (Cover and Thomas 2005), as well as approaches to diagnose how unique the information provided by new data sources is relative to others (Goodwell and Kumar 2017, Williams and Beer 2010). This study addresses three related questions: (1) Do new observations (here δ^2H , $\delta^{18}O$, and $\delta^{13}C$ values) contain useful information about the bulk *NEE* and *LH* fluxes across North America? (2) Can any of the information provided by new (isotope) measurements be obtained from other meteorological variables? And (3) under which environmental conditions do these new measurements provide the most additional information? In doing so, this study provides a generalizable approach for evaluating the conditions under which novel geoscience data is helpful for understanding the Earth system. It also formally quantifies the conditions under which environmental processes associated with transformations of stable isotope ratios, as measured systematically within continental scale networks, are a greater contribution to overall environmental exchanges. This approach thereby provides key process level benchmarks for advancing research into Earth's integrated carbon and water cycles.

2 Materials and methods

2.1 Study sites and data preparations

This study was conducted at terrestrial sites that are part of the United States National Ecological Observatory Network (NEON), which is a continental scale research platform for understanding the ecological responses to climate change, land use change, and species invasion (Barnett *et al* 2019). We used the 30-minute aggregated *NEE*, *LH*, global radiation (R_g), air temperature (T), and the two-dimensional wind speed (u) datasets from the NEON's eddy covariance bundled datasets (NEON 2022a). The vapor pressure deficit (*VPD*) data were derived based on NEON's relative humidity, temperature, and barometric pressure products (NEON 2022b). The *NEE* and *LH* data were filtered for periods of low turbulence based on friction velocities (u^*) then gap-filled using the marginal distribution sampling method (Wutzler *et al* 2018). The gap-filled and u^* filtered 30-minute fluxes were further averaged on a daily scale to facilitate future analysis. All 30-minute meteorological variables except wind speed were gap-filled using the marginal distribution sampling mentioned above. The gap-filled meteorological variables were then averaged to daily scale. Extreme values in daily flux and meteorological datasets were further processed using an inter-quantile filter (Goodwell and Kumar 2017). More details can be found in Supplemental information. Daily stable isotope ratios (δ^2H , $\delta^{18}O$, and $\delta^{13}C$) of *NEE* and *LH* were obtained from a recently published dataset (Finkenbiner *et al* 2022), which was derived based on the isotope composition of carbon dioxide and water vapor from EC tower profiles across NEON sites. The $\delta^{18}O$ values were converted to deuterium excess (d) via $d = \delta^2H - 8 * \delta^{18}O$ (Dansgaard 1964).

2.2 Information measures

In this study the mutual information metric, $I(X;Y)$, was chosen to analyze how different meteorological variables share information about ecosystem fluxes because it has the advantage over traditional metric (e.g., correlation coefficient) of capturing both linear and non-linear dependencies between two variables. It represents the reduction in uncertainties of one variable given the knowledge of another variable. Formally, mutual information is a measure of how two random variables are probabilistically dependent on each other in the unit of bits (Cover and Thomas 2005). Probabilistically, the mutual information can be expressed as:

$$I(X;Y) = \sum p(x,y) \log_2 \left(\frac{p(x,y)}{p(x)p(y)} \right) \quad (1)$$

where $p(x)$, $p(y)$, and $p(x,y)$ are the probability density functions of random variables X , Y , and $\{X,Y\}$ respectively.

The multivariate mutual information, $I(X,Y;Z)$, of a single random variable (Z) and a set of random variables $\{X, Y\}$ characterizes the amount of uncertainty in Z that can be reduced by the knowledge of $\{X, Y\}$ and can be expressed as:

$$I(X,Y;Z) = \sum p(x,y,z) \log_2 \left(\frac{p(x,y,z)}{p(x,y)p(z)} \right) \quad (2)$$

where $p(z)$, $p(x,y)$, and $p(x,y,z)$ are the probability density functions of variables Z , $\{X,Y\}$, and $\{X,Y,Z\}$, respectively and were estimated using a kernel density estimation (KDE) method with a gaussian kernel and Silverman bandwidth selection method (Silverman 2018). To evaluate the above information metrics, we rescaled each data point to a common range of [0, 1] before using KDE. We then evaluate the probability density functions from 0 to 1 with a step size of 0.05.

We computed the pairwise mutual information (e.g., $I(VPD;NEE)$, $I(VPD;LH)$, etc.) shared among VPD , T , R_g , u , $\delta^{13}C$, δ^2H , and d about NEE and LH iteratively. Due to the limitation of isotope datasets, we computed the mutual information of each variable with the NEE and LH by subsampling 100 data points without replacement 500 times to ensure equal constituent data counts in mutual information calculations. Then, the mutual information of the variable of interest and the flux is computed as the average mutual information across 500 resamplings. The mutual information contents computed above are evaluated for statistical significance (refer to Supplemental information for details).

2.3 Partial information decomposition

The multivariate mutual information can be decomposed into different informational components via a partial information decomposition framework (PID) (Goodwell and Kumar 2017, Goodwell et al 2018, Williams and Beer 2010). This framework captures how the different source variables interactively influence a target variable of interest, which can possibly reveal the process that relates source variables and a target without any modeling assumptions. The PID can decompose $I(X,Y;Z)$ into: (1) unique information (U) that is only provided by X or Y solely to Z ; (2) synergistic information (S) that is the information provided to the Z when X and Y act jointly; (3) redundant

information (R) that is the overlapping information provided both by X and Y to the Z (Goodwell and Kumar 2017). The PID framework can be formulated as

$$I(X,Y; Z) = U_X + U_Y + R + S \quad (3)$$

$$I(X; Z) = U_X + R \quad (4)$$

$$I(Y; Z) = U_Y + R \quad (5)$$

Where U_X and U_Y are the unique information of X and Y to Z, respectively. R and S are the redundant and synergistic information of X and Y to Z, respectively. All PID components are non-negative real numbers in unit of bits (Goodwell and Kumar 2017).

In this study, we quantified the information flow between each flux and each isotope ratio by leveraging the PID framework (Goodwell and Kumar 2017). We defined the decomposed information components that the isotope ratios provided to the bulk fluxes as the averaged unique information across all meteorological variables (VPD , T , R_g , and u). As with computing the individual mutual information, we also subsampled 100 data points from each dataset without replacement 500 times. The partial information components of the isotopes were then computed as the averaged information components from 500 iterations. The significance tests were performed similarly to mutual information (refer to Supplemental information for details).

3. Results

Informational analysis shows that isotope data ($\delta^{13}C$, δ^2H , and d) and traditional meteorological data (R_g , T , VPD , u) each contain significant information about temporal variation in NEE and LH fluxes (Fig. 1). This formally demonstrates that NEE and LH become less uncertain given the knowledge of isotope data or meteorological data throughout the NEON sites. We find that R_g , T , and VPD observations consistently contain more information about environmental fluxes than the isotope data products. This analysis shows that wind speed (u) provides comparable amount information about NEE and LH fluxes (Fig. 1) as the isotope data. Though the information provided by R_g , T , and VPD is larger than the information from u and the isotopes, u is nevertheless one of the well-established drivers of surface-atmosphere water and carbon exchange and is commonly measured at meteorological stations worldwide (Yusup and Liu 2020).

In general, individual variables tend to share more information with LH than NEE (Fig. 1). This indicates that LH is generally more easily constrained and predicted based on these environmental observations, possibly because it more strongly captures isotopic differences in the contributing one-way flux compared to NEE which is the net sum of two opposing fluxes with less distinct isotope ratios. Instead of $\delta^{13}C$ values best constraining NEE and δ^2H or d values best constraining LH , we find that δ^2H values on average provide slightly more mutual information than $\delta^{13}C$ values for both NEE and LH fluxes; however, both these (i.e., δ^2H and $\delta^{13}C$) are more informative than d . NEE is a

quantity that encompasses downward carbon uptake via plant photosynthesis and carbon release upward through respiration (Reichstein *et al* 2005) while water, as represented by LH , is evaporated upward during evapotranspiration. δ^2H links with the phase transformation of water that is strongly temperature dependent (Xiao *et al* 2018). Therefore, δ^2H is more likely to carry slightly more information about LE and NEE than $\delta^{13}C$. The amount of information that can be inferred from isotopes (and other variables) about NEE and LH is highly unlikely to be obtained by random processes ($p < 0.01$).

We decomposed and evaluated the multivariate mutual information between environmental fluxes, isotope ratios, and other variables (Fig. 2). These results demonstrate that most of the information provided by the isotopes about NEE and LH is unique to these measurements ($\delta^{13}C$ and δ^2H). This unique information (i.e., the information contribution that is contributed only by one variable to the target variable) provided by $\delta^{13}C$ and δ^2H values about LH is generally higher than the unique information provided about NEE . The unique information provided by $\delta^{13}C$ and δ^2H values is higher than that contained within d values for both LH and NEE fluxes. The unique information is found to vary spatially across the NEON sites (Supplemental Fig. S1). All the unique information provided by the isotope ratios is statistically significant and highly unlikely to be obtained at random ($p < 0.01$).

In addition to the unique information that $\delta^{13}C$, δ^2H , and d values contain about NEE and LH fluxes, a smaller amount of synergistic (i.e., the information component when isotope and other variables act jointly to provide information about ecosystem fluxes) and redundant information (i.e., the overlapping information that isotope or other variables contribute to ecosystem fluxes) is also presented (Supplemental Fig. S2 and S3). Among all the isotope measurements, the synergistic component of d values is slightly larger for NEE . In general, redundant information tends to be smaller than the unique and synergistic components. The unique and redundant information linking isotopes with NEE and LH are statistically significant ($p < 0.01$).

The total additional information, represented by the sum of the synergistic information and the unique information ($U+S$), provided by each flux isotope composition to LH and NEE varies spatially across NEON sites (Fig. 3). $\delta^{13}C$ contributes the most substantial information about NEE and LH in the Northeastern US (i.e., New Hampshire) and southwestern US (i.e., New Mexico), respectively (Fig. 3a and Fig. 3d). In northern Alaska, δ^2H contributes the largest amount of additive information to NEE (Fig. 3b). There is an increased possibility of observing more additive information of δ^2H about LH at site with higher latitude (Fig. 3e). The highest additional that d provides to NEE and LH were observed in Virginia (Fig. 3c) and Wyoming (Fig. 3f), respectively. The fraction of the total information for isotopes ($U+S+R$) about NEE that is additive, i.e. $(U+S)/(U+S+R)$, is 0.95 for $\delta^{13}C$, 0.92 for δ^2H , and 0.99 for d , respectively). For LH , δ^2H and $\delta^{13}C$ provided more additive information than d (Fig. 3d-f). The fraction of additive information about LH is 0.89 for $\delta^{13}C$, 0.84 for δ^2H , and 0.94 for d , respectively. The additive information of $\delta^{13}C$, δ^2H , and d relating to LH has larger variability among sites

than that relating to *NEE* (Fig. 3). All the additive information of these isotopes relating to *NEE* and *LH* is statistically significant ($p < 0.01$).

4. Discussion

Our analysis provides a rigorous evaluation of the quantitative value of isotope ratios to provide useful information about carbon and water fluxes across continental scale gradients. For these bulk fluxes, we showed that the information individually provided by these isotopes was similar to the amount of information provided by wind speed measurements, while providing less information than atmospheric vapor pressure deficit, air temperature, and radiation measurements (Fig. 1). The meteorological observations evaluated here are commonly used to drive forecasts of environmental processes (Cosgrove *et al* 2003, Rodell *et al* 2004) and thus serve as a benchmark for environmental data. A prior *NEE* simulation showed that radiation was consistently the most sensitive predictor for the simulation of *NEE* at maize fields with distinct irrigation practices (Safa *et al* 2019). Similarly, a sensitivity analysis on global evapotranspiration models indicated that net radiation was one of the influential input variables (Talsma *et al* 2018). Our results are consistent with the fundamental notion that solar radiation is the basis for all ecosystem functions (Yetemen *et al* 2015) (excluding rare energy transformations) and drives most diurnal variation in air temperature and vapor pressure deficit and therefore is more likely to share higher amount of mutual information individually with *LH* and *NEE*, with temperature and moisture levels of secondary importance and isotope metrics and wind speed of tertiary importance.

The meteorological variables evaluated here are known to be inter-related to some extent. For instance, the vapor pressure deficit is strongly dependent on air temperature due to the Clausius-Clapeyron relationship (Clausius 1850) and air temperature is tightly related to the amount of radiation as well as to sensible heat fluxes. Past studies have highlighted how *NEE* and *LH* respond to changes in vapor pressure deficit, air temperature and radiation across various scales, seasons, and ecosystems (Chen *et al* 2020, Niu *et al* 2012, Gu *et al* 2006). Vapor pressure deficit was found to have direct effect on surface energy partitioning as high vapor pressure deficit represents high atmosphere demand and hence high *LH* with constant surface conductance (Tong *et al* 2022, Wang *et al* 2019). Yet, high vapor pressure deficit can reduce stomatal conductance and thereby reduce plant photosynthesis (Grossiord *et al* 2020). Wind speed can modulate the rate of evapotranspiration and thereby *LH* (Yang *et al* 2019, Liu and Zhang 2013). The different effect of vapor pressure deficit and wind speed on *LH* may be underrepresented by other metrics but can be captured if evaluated using information theory-based metrics like those explored here.

Information carried by these isotope ratios was found to be distinct from the traditional meteorological variables examined here. It is also crucial to understand how different

variables interactively provide information to a target of interest because knowledge of the interdependencies between the inputs and outputs of a studied system is fundamental for model uncertainty characterization (Ruddell *et al* 2019, Li and Good 2021, Gong *et al* 2013). In fact, one of the challenges for land surface models is increasing process complexity with the integration of a set of sub-models with the expansion of input dimensions (Fisher and Koven 2020), which can increase the risk of model “equifinality”. Moreover, numerous models have been developed to estimate ecosystem fluxes (Wood 2021, Su 2002, Veroustraete *et al* 1996). However, these methods often require some assumptions or simplifications, which can be subject to significant uncertainty (Papale *et al* 2006, Zhao *et al* 2020). In general, it may be more desirable for each of the inputs in a model to provide unique or synergistic pieces of information (Wibral *et al* 2017), which can potentially capture different processes relating to the target (Goodwell *et al* 2018). Therefore, the construction and simplification of ecosystem models should move towards a direction that maximizes unique information provided by each input.

The decomposition of the multivariate mutual information between isotopes, other meteorological variables, and the bulk fluxes offers an opportunity to elucidate how much of the information from isotopes is transferred to the bulk fluxes (*NEE* and *LH*). In this study, the portion of unique information from isotopes measurements for carbon and water isotopes was statistically significant. This suggests that processes driving variation in isotope ratios may influence these fluxes via distinct pathways. We observed inter-site variations in the unique information provided by the isotopes, indicating that the unique information may be dependent on site-specific conditions such as aridity and precipitation. There is a higher chance that $\delta^{13}\text{C}$ contributes more information about *LH* under drier or lower precipitation conditions (Supplemental Fig. S4). Additionally, both $\delta^{13}\text{C}$ and $\delta^2\text{H}$ tend to provide more distinct insights into *NEE* and *LH* in cooler or lower precipitation conditions. This suggests that the patterns of bulk fluxes can potentially be better characterized and predicted with the isotopes included as an additional constraint.

The additional information provided by isotopes to these bulk fluxes are described by the sum of unique information and synergistic information. Our analysis demonstrates that fusing isotope data products with more traditional datasets can potentially lead to better monitoring and prediction of *NEE* and *LH* in a process modeling framework, as these isotope datasets provide additional information beyond traditional meteorological variables and are associated with known physical mechanisms. The incorporation of isotope datasets into artificial intelligence (AI) and machine learning (ML) models, especially explainable AI models, can potentially improve predictive accuracies and enhance our understanding of ecosystem fluxes. Nevertheless, uncertainties can be introduced when incorporating isotope dataset to models with larger spatial scale. It is challenging to include isotope datasets to models that require larger spatial scale isotope datasets, as they are often hard to acquire. Researchers might also consider different incorporation strategies in different ecoclimate regions. In addition, the amount

of added information of the isotope datasets is likely to vary across sites, climate, and ecosystems. To assess this, we evaluated the additive information of isotopes based on NEON site conditions via a simple linear regression analysis (Fig. 4). We showed that the additive information that $\delta^{13}\text{C}$ provides about LH is influenced by mean annual precipitation, aridity, and site elevation (Fig. 4d), as indicated by a significant slope value from the linear regression. $\delta^{13}\text{C}$ is likely to provide more useful information about LH in locations with higher atmospheric evaporative demand relative to precipitation, or in locations with less annual precipitation or with higher altitude. The additive information δ^2H provides about NEE was shown to be mainly influenced by the site mean annual temperature (Fig. 4b). δ^2H tends to be more informative about NEE in locations with cooler climates. Similarly, there is more opportunity for δ^2H to provide additional knowledge about LH at locations with cooler climates or less mean annual precipitation (Fig. 4e). No significant relationship was found between the additional information of the d provided to either NEE or LH .

Variations in additional information across NEON sites indicate differences in conditional dependencies of ecosystem fluxes on processes related to isotope fluxes. Changes in ecosystem structure and climate affect the ecosystem's adaptability to environmental changes (Weiskopf *et al* 2020) that influences the biochemical processes responsible for isotope fractionation, which can intensify or weaken these conditional dependencies. It's worth noting that this study primarily examined how each isotope contributes additional information to NEE and LH with an emphasis on atmospheric centric conditions. However, it is crucial to acknowledge that ecosystems broadly have a wide range of inherent complexities, such as geomorphology (e.g., slope, aspect) subsurface dynamics (e.g., depth to water table), vegetation species and traits (e.g. plant hydraulic traits), and soil physics (e.g., soil texture), which might play a role in shaping the way of how isotope observations provide extra information about NEE and LH .

One of key motivations for measuring stable isotopes of water and carbon fluxes is that they may provide unique and novel knowledge about key mechanisms across ecosystems (Good *et al* 2014, Conrad *et al* 2012, Wang *et al* 2010). Such hypothesis has not been formally tested until this study. This is because the flux isotope ratios are influenced by distinct biophysical processes, and thus larger amounts of new mutual information between isotopes and environmental fluxes quantifies the conditions under which these processes are more dominant components of overall bulk fluxes. In this light, the trends described above (and in Fig. 4) are consistent with prior knowledge of isotope geophysics. For instance, equilibrium fractionation factors are sensitive to temperature, particularly at low values (Bowen and Good 2015), with broad decreases in vapor δ^2H observed poleward at continental scales (Good *et al* 2015). Similarly, evaporation is expected to play a larger role in LH fluxes under low vegetation, more arid climates (Wang *et al* 2014) , and this study provides a new way to quantify the relative importance of these isotope processes on bulk fluxes.

It is important to acknowledge that our analysis focused on how daily isotope datasets are informative of bulk ecosystem fluxes. It might be worthwhile to analyze how similar observations are informative of ecosystem fluxes at finer temporal scales. For instance, how lags in isotope dataset responses are influenced ecosystem processes, and correspondingly how do the partial information components change with different lag timescales can possibly reveal more detailed linkages between ecosystem fluxes and isotope fluxes. In this study, we considered abiotic variables (VPD , T , u , R_g) as the confounding part in the partial information decomposition. It might also be worthwhile to explore how other biotic variables such as ecosystem structure, species composition, and plant hydraulic traits, rooting depth can influence the total additive information of isotope dataset to the bulk fluxes.

This analysis is based on current available data products and quality control methods. As more NEON data becomes available, future studies to may investigate if and how the results vary with longer timeseries data and a wider range of environmental conditions. However, given the power of isotopes for tackling fundamental problems in carbon and water cycling and projecting the future of terrestrial ecosystem function under a rapidly changing climate (Bowen and Good 2015, Bowling *et al* 2008), our results can be useful to provide guidance for improving model results after the incorporation of isotope flux ratios.

Acknowledgements

The authors want to acknowledge the funding support of the United States National Science Foundation (DEB1802885 and DEB1802880). RPF also received support from the Laboratory Directed Research and Development program of Los Alamos National Laboratory under project number 20210961PRD3.

Author contribution

BL and SPG designed the study. RPF provided flux datasets and gap-filled meteorological datasets and wrote part of the data processing steps in Supplementary material. BL analyzed the data and wrote the manuscript. SPG, RPF, CEF, GJB, DCN, CJS, and WRLA reviewed the manuscript.

Data availability statement

The datasets that are associated with this study is publicly available at <https://data.neonscience.org/> and <https://www.hydroshare.org/resource/e74edc35d45441579d51286ea01b519f/>. All

414 materials associated with this study will be made available at
415 https://github.com/libonancaesar/ERL_info_isotope

416

417 **Competing interest statement**

418 The authors declare no conflicts of interest.

419

420

References

- Baldocchi D 2014 Measuring fluxes of trace gases and energy between ecosystems and the atmosphere - the state and future of the eddy covariance method *Glob Chang Biol* **20** 3600–9 Online: <https://onlinelibrary.wiley.com/doi/10.1111/gcb.12649>
- Barnett D T, Adler P B, Chemel B R, Duffy P A, Enquist B J, Grace J B, Harrison S, Peet R K, Schimel D S, Stohlgren T J and Vellend M 2019 The plant diversity sampling design for The National Ecological Observatory Network *Ecosphere* **10** Online: <https://onlinelibrary.wiley.com/doi/10.1002/ecs2.2603>
- Berkelhammer M, Hu J, Bailey A, Noone D C, Still C J, Barnard H, Gochis D, Hsiao G S, Rahn T and Turnipseed A 2013 The nocturnal water cycle in an open-canopy forest *Journal of Geophysical Research: Atmospheres* **118** 10,225–10,242 Online: <http://doi.wiley.com/10.1002/jgrd.50701>
- Bowen G J and Good S P 2015 Incorporating water isoscapes in hydrological and water resource investigations *WIREs Water* **2** 107–19 Online: <https://onlinelibrary.wiley.com/doi/10.1002/wat2.1069>
- Bowling D R, Pataki D E and Randerson J T 2008 Carbon isotopes in terrestrial ecosystem pools and CO₂ fluxes *New Phytologist* **178** 24–40 Online: <https://onlinelibrary.wiley.com/doi/10.1111/j.1469-8137.2007.02342.x>
- Chen J, Wen J, Kang S, Meng X, Tian H, Ma X and Yuan Y 2020 Assessments of the factors controlling latent heat flux and the coupling degree between an alpine wetland and the atmosphere on the Qinghai-Tibetan Plateau in summer *Atmos Res* **240** 104937 Online: <https://linkinghub.elsevier.com/retrieve/pii/S016980951931573X>
- Clausius R 1850 Ueber die bewegende Kraft der Wärme und die Gesetze, welche sich daraus für die Wärmelehre selbst ableiten lassen *Annalen der Physik und Chemie* **155** 500–24 Online: <https://onlinelibrary.wiley.com/doi/10.1002/andp.18501550403>
- Conrad R, Klose M, Yuan Q, Lu Y and Chidthaisong A 2012 Stable carbon isotope fractionation, carbon flux partitioning and priming effects in anoxic soils during methanogenic degradation of straw and soil organic matter *Soil Biol Biochem* **49** 193–9 Online: <https://linkinghub.elsevier.com/retrieve/pii/S0038071712000958>
- Cosgrove B A, Lohmann D, Mitchell K E, Houser P R, Wood E F, Schaake J C, Robock A, Marshall C, Sheffield J, Duan Q, Luo L, Higgins R W, Pinker R T, Tarpley J D and Meng J 2003 Real-time and retrospective forcing in the North American Land Data Assimilation System (NLDAS) project *Journal of Geophysical Research: Atmospheres* **108** 2002JD003118 Online: <https://onlinelibrary.wiley.com/doi/abs/10.1029/2002JD003118>

458 Cover T M and Thomas J A 2005 *Elements of Information Theory* (Wiley) Online:
 459 <https://onlinelibrary.wiley.com/doi/book/10.1002/047174882X>

460 Dansgaard W 1964 Stable isotopes in precipitation *Tellus A: Dynamic Meteorology and*
 461 *Oceanography* **16** 436–68

462 Dubbert M and Werner C 2019 Water fluxes mediated by vegetation: emerging isotopic
 463 insights at the soil and atmosphere interfaces *New Phytologist* **221** 1754–63 Online:
 464 <https://onlinelibrary.wiley.com/doi/10.1111/nph.15547>

465 Finkenbiner C E, Li B, Spencer L, Butler Z, Haagsma M, Fiorella R P, Allen S T,
 466 Anderegg W, Still C J, Noone D, Bowen G J and Good S P 2022 The NEON Daily
 467 Isotopic Composition of Environmental Exchanges Dataset *Sci Data* **9** 353 Online:
 468 <https://www.nature.com/articles/s41597-022-01412-4>

469 Fiorella R P, Good S P, Allen S T, Guo J S, Still C J, Noone D C, Anderegg W R L,
 470 Florian C R, Luo H, Pingingtha-Durden N and Bowen G J 2021 Calibration
 471 Strategies for Detecting Macroscale Patterns in NEON Atmospheric Carbon
 472 Isotope Observations *J Geophys Res Biogeosci* **126**

473 Fisher R A and Koven C D 2020 Perspectives on the Future of Land Surface Models
 474 and the Challenges of Representing Complex Terrestrial Systems *J Adv Model*
 475 *Earth Syst* **12** Online: <https://onlinelibrary.wiley.com/doi/10.1029/2018MS001453>

476 Gemery P A, Trolier M and White J W C 1996 Oxygen isotope exchange between
 477 carbon dioxide and water following atmospheric sampling using glass flasks
 478 *Journal of Geophysical Research: Atmospheres* **101** 14415–20

479 Gong W, Gupta H V., Yang D, Sricharan K and Hero A O 2013 Estimating epistemic
 480 and aleatory uncertainties during hydrologic modeling: An information theoretic
 481 approach *Water Resour Res* **49** 2253–73 Online:
 482 <http://doi.wiley.com/10.1002/wrcr.20161>

483 Good S P, Noone D, Kurita N, Benetti M and Bowen G J 2015 D/H isotope ratios in the
 484 global hydrologic cycle *Geophys Res Lett* **42** 5042–50 Online:
 485 <http://doi.wiley.com/10.1002/2015GL064117>

486 Good S P, Soderberg K, Guan K, King E G, Scanlon T M and Caylor K K 2014 $\delta^2\text{H}$
 487 isotopic flux partitioning of evapotranspiration over a grass field following a water
 488 pulse and subsequent dry down *Water Resour Res* **50** 1410–32 Online:
 489 <http://doi.wiley.com/10.1002/2013WR014333>

490 Goodwell A E and Kumar P 2017 Temporal information partitioning: Characterizing
 491 synergy, uniqueness, and redundancy in interacting environmental variables *Water*
 492 *Resour Res* **53** 5920–42 Online:
 493 <https://onlinelibrary.wiley.com/doi/10.1002/2016WR020216>

494 Goodwell A E, Kumar P, Fellows A W and Flerchinger G N 2018 Dynamic process
 495 connectivity explains ecohydrologic responses to rainfall pulses and drought
 496 *Proceedings of the National Academy of Sciences* **115** Online:
 497 <https://pnas.org/doi/full/10.1073/pnas.1800236115>

498 Grossiord C, Buckley T N, Cernusak L A, Novick K A, Poulter B, Siegwolf R T W, Sperry
 499 J S and McDowell N G 2020 Plant responses to rising vapor pressure deficit *New*
 500 *Phytologist* **226** 1550–66 Online:
 501 <https://onlinelibrary.wiley.com/doi/10.1111/nph.16485>

502 Gu L, Meyers T, Pallardy S G, Hanson P J, Yang B, Heuer M, Hosman K P, Riggs J S,
 503 Sluss D and Wullschlegel S D 2006 Direct and indirect effects of atmospheric
 504 conditions and soil moisture on surface energy partitioning revealed by a prolonged
 505 drought at a temperate forest site *J Geophys Res* **111** D16102 Online:
 506 <http://doi.wiley.com/10.1029/2006JD007161>

507 Guan K, Berry J A, Zhang Y, Joiner J, Guanter L, Badgley G and Lobell D B 2016
 508 Improving the monitoring of crop productivity using spaceborne solar-induced
 509 fluorescence *Glob Chang Biol* **22** 716–26 Online:
 510 <https://onlinelibrary.wiley.com/doi/10.1111/gcb.13136>

511 Jia Z, Liu S, Xu Z, Chen Y and Zhu M 2012 Validation of remotely sensed
 512 evapotranspiration over the Hai River Basin, China *Journal of Geophysical*
 513 *Research: Atmospheres* **117** n/a-n/a Online:
 514 <http://doi.wiley.com/10.1029/2011JD017037>

515 Jung M, Reichstein M, Margolis H A, Cescatti A, Richardson A D, Arain M A, Arneeth A,
 516 Bernhofer C, Bonal D, Chen J, Gianelle D, Gobron N, Kiely G, Kutsch W, Lasslop
 517 G, Law B E, Lindroth A, Merbold L, Montagnani L, Moors E J, Papale D,
 518 Sottocornola M, Vaccari F and Williams C 2011 Global patterns of land-atmosphere
 519 fluxes of carbon dioxide, latent heat, and sensible heat derived from eddy
 520 covariance, satellite, and meteorological observations *J Geophys Res* **116** G00J07
 521 Online: <http://doi.wiley.com/10.1029/2010JG001566>

522 Lee S-C, Christen A, Black T A, Jassal R S, Ketler R and Nesic Z 2020 Partitioning of
 523 net ecosystem exchange into photosynthesis and respiration using continuous
 524 stable isotope measurements in a Pacific Northwest Douglas-fir forest ecosystem
 525 *Agric For Meteorol* **292–293** 108109 Online:
 526 <https://linkinghub.elsevier.com/retrieve/pii/S0168192320302112>

527 Li B and Good S P 2021 Information-based uncertainty decomposition in dual-channel
 528 microwave remote sensing of soil moisture *Hydrol Earth Syst Sci* **25** 5029–45
 529 Online: <https://hess.copernicus.org/articles/25/5029/2021/>

530 Li S, Kang S, Li F and Zhang L 2008 Evapotranspiration and crop coefficient of spring
 531 maize with plastic mulch using eddy covariance in northwest China *Agric Water*

532 *Manag* **95** 1214–22 Online:
 533 <https://linkinghub.elsevier.com/retrieve/pii/S0378377408001169>

534 Liu X and Zhang D 2013 Trend analysis of reference evapotranspiration in Northwest
 535 China: The roles of changing wind speed and surface air temperature *Hydrol*
 536 *Process* **27** 3941–8 Online: <https://onlinelibrary.wiley.com/doi/10.1002/hyp.9527>

537 Lupascu M, Akhtar H, Smith T E L and Sukri R S 2020 Post-fire carbon dynamics in the
 538 tropical peat swamp forests of Brunei reveal long-term elevated CH₄ flux *Glob*
 539 *Chang Biol* **26** 5125–45 Online:
 540 <https://onlinelibrary.wiley.com/doi/10.1111/gcb.15195>

541 National Ecological Observatory Network (NEON) 2022a Bundled data products - eddy
 542 covariance (DP4.00200.001) Online: <https://data.neonscience.org>

543 National Ecological Observatory Network (NEON) 2022b Relative humidity
 544 (DP1.00098.001) Online: <https://data.neonscience.org>

545 Niu S, Luo Y, Fei S, Yuan W, Schimel D, Law B E, Ammann C, Altaf Arain M, Arneth A,
 546 Aubinet M, Barr A, Beringer J, Bernhofer C, Andrew Black T, Buchmann N,
 547 Cescatti A, Chen J, Davis K J, Dellwik E, Desai A R, Etzold S, Francois L, Gianelle
 548 D, Gielen B, Goldstein A, Groenendijk M, Gu L, Hanan N, Helfter C, Hirano T,
 549 Hollinger D Y, Jones M B, Kiely G, Kolb T E, Kutsch W L, Lafleur P, Lawrence D M,
 550 Li L, Lindroth A, Litvak M, Loustau D, Lund M, Marek M, Martin T A, Matteucci G,
 551 Migliavacca M, Montagnani L, Moors E, William Munger J, Noormets A, Oechel W,
 552 Olejnik J, U K T P, Pilegaard K, Rambal S, Raschi A, Scott R L, Seufert G, Spano
 553 D, Stoy P, Sutton M A, Varlagin A, Vesala T, Weng E, Wohlfahrt G, Yang B, Zhang
 554 Z and Zhou X 2012 Thermal optimality of net ecosystem exchange of carbon
 555 dioxide and underlying mechanisms *New Phytologist* **194** 775–83 Online:
 556 <https://onlinelibrary.wiley.com/doi/10.1111/j.1469-8137.2012.04095.x>

557 Orlowski N, Breuer L, Angeli N, Boeckx P, Brumbt C, Cook C S, Dubbert M, Dyckmans
 558 J, Gallagher B, Gralher B, Herbstritt B, Hervé-Fernández P, Hissler C, Koeniger P,
 559 Legout A, Macdonald C J, Oyarzún C, Redelstein R, Seidler C, Siegwolf R, Stumpp
 560 C, Thomsen S, Weiler M, Werner C and McDonnell J J 2018 Inter-laboratory
 561 comparison of cryogenic water extraction systems for stable isotope analysis of soil
 562 water *Hydrol Earth Syst Sci* **22** 3619–37

563 Papale D, Reichstein M, Aubinet M, Canfora E, Bernhofer C, Kutsch W, Longdoz B,
 564 Rambal S, Valentini R, Vesala T and Yakir D 2006 Towards a standardized
 565 processing of Net Ecosystem Exchange measured with eddy covariance technique:
 566 algorithms and uncertainty estimation *Biogeosciences* **3** 571–83 Online:
 567 <https://bg.copernicus.org/articles/3/571/2006/>

568 Piao S, Wang X, Wang K, Li X, Bastos A, Canadell J G, Ciais P, Friedlingstein P and
 569 Sitch S 2020 Interannual variation of terrestrial carbon cycle: Issues and

570 perspectives *Glob Chang Biol* **26** 300–18 Online:
 571 <https://onlinelibrary.wiley.com/doi/10.1111/gcb.14884>

572 Reichstein M, Falge E, Baldocchi D, Papale D, Aubinet M, Berbigier P, Bernhofer C,
 573 Buchmann N, Gilmanov T, Granier A, Grunwald T, Havrankova K, Ilvesniemi H,
 574 Janous D, Knohl A, Laurila T, Lohila A, Loustau D, Matteucci G, Meyers T, Miglietta
 575 F, Ourcival J-M, Pumpanen J, Rambal S, Rotenberg E, Sanz M, Tenhunen J,
 576 Seufert G, Vaccari F, Vesala T, Yakir D and Valentini R 2005 On the separation of
 577 net ecosystem exchange into assimilation and ecosystem respiration: review and
 578 improved algorithm *Glob Chang Biol* **11** 1424–39 Online:
 579 <https://onlinelibrary.wiley.com/doi/10.1111/j.1365-2486.2005.001002.x>

580 Rodell M, Houser P R, Jambor U, Gottschalck J, Mitchell K, Meng C-J, Arsenault K,
 581 Cosgrove B, Radakovich J, Bosilovich M, Entin J K, Walker J P, Lohmann D and
 582 Toll D 2004 The Global Land Data Assimilation System *Bull Am Meteorol Soc* **85**
 583 381–94 Online: <https://journals.ametsoc.org/doi/10.1175/BAMS-85-3-381>

584 Ruddell B L, Drewry D T and Nearing G S 2019 Information Theory for Model
 585 Diagnostics: Structural Error is Indicated by Trade-Off Between Functional and
 586 Predictive Performance *Water Resour Res* **55** 6534–54 Online:
 587 <https://onlinelibrary.wiley.com/doi/10.1029/2018WR023692>

588 Safa B, Arkebauer T J, Zhu Q, Suyker A and Irmak S 2019 Net Ecosystem Exchange
 589 (NEE) simulation in maize using artificial neural networks *IFAC Journal of Systems*
 590 *and Control* **7** 100036 Online:
 591 <https://linkinghub.elsevier.com/retrieve/pii/S2468601817302584>

592 Schimel D and Schneider F D 2019 Flux towers in the sky: global ecology from space
 593 *New Phytologist* **224** 570–84 Online:
 594 <https://onlinelibrary.wiley.com/doi/10.1111/nph.15934>

595 Silverman B W 2018 *Density Estimation for Statistics and Data Analysis* (Routledge)
 596 Online: <https://www.taylorfrancis.com/books/9781351456173>

597 Still C J, Rastogi B, Page G F M, Griffith D M, Sibley A, Schulze M, Hawkins L, Pau S,
 598 Detto M and Helliker B R 2021 Imaging canopy temperature: shedding (thermal)
 599 light on ecosystem processes *New Phytologist* **230** 1746–53 Online:
 600 <https://onlinelibrary.wiley.com/doi/10.1111/nph.17321>

601 Su Z 2002 The Surface Energy Balance System (SEBS) for estimation of turbulent heat
 602 fluxes *Hydrol Earth Syst Sci* **6** 85–100 Online:
 603 <https://hess.copernicus.org/articles/6/85/2002/>

604 Talsma C, Good S, Miralles D, Fisher J, Martens B, Jimenez C and Purdy A 2018
 605 Sensitivity of Evapotranspiration Components in Remote Sensing-Based Models
 606 *Remote Sens (Basel)* **10** 1601 Online: <http://www.mdpi.com/2072-4292/10/10/1601>

607 Tong B, Guo J, Xu H, Wang Y, Li H, Bian L, Zhang J and Zhou S 2022 Effects of soil
608 moisture, net radiation, and atmospheric vapor pressure deficit on surface
609 evaporation fraction at a semi-arid grass site *Science of The Total Environment* **849**
610 157890 Online: <https://linkinghub.elsevier.com/retrieve/pii/S0048969722049890>

611 URycki D R, Bassiouni M, Good S P, Crump B C and Li B 2022 The streamwater
612 microbiome encodes hydrologic data across scales *Science of The Total*
613 *Environment* **849** 157911 Online:
614 <https://linkinghub.elsevier.com/retrieve/pii/S0048969722050100>

615 Veroustraete F, Patyn J and Myneni R B 1996 Estimating net ecosystem exchange of
616 carbon using the normalized difference vegetation index and an ecosystem model
617 *Remote Sens Environ* **58** 115–30 Online:
618 <https://linkinghub.elsevier.com/retrieve/pii/0034425795002588>

619 Wang L, Caylor K K, Villegas J C, Barron-Gafford G A, Breshears D D and Huxman T E
620 2010 Partitioning evapotranspiration across gradients of woody plant cover:
621 Assessment of a stable isotope technique *Geophys Res Lett* **37** n/a-n/a Online:
622 <http://doi.wiley.com/10.1029/2010GL043228>

623 Wang L, Good S P and Caylor K K 2014 Global synthesis of vegetation control on
624 evapotranspiration partitioning *Geophys Res Lett* **41** 6753–7 Online:
625 <http://doi.wiley.com/10.1002/2014GL061439>

626 Wang P, Li D, Liao W, Rigden A and Wang W 2019 Contrasting Evaporative
627 Responses of Ecosystems to Heatwaves Traced to the Opposing Roles of Vapor
628 Pressure Deficit and Surface Resistance *Water Resour Res* **55** 4550–63 Online:
629 <https://onlinelibrary.wiley.com/doi/10.1029/2019WR024771>

630 Weiskopf S R, Rubenstein M A, Crozier L G, Gaichas S, Griffis R, Halofsky J E, Hyde K
631 J W, Morelli T L, Morissette J T, Muñoz R C, Pershing A J, Peterson D L, Poudel R,
632 Staudinger M D, Sutton-Grier A E, Thompson L, Vose J, Weltzin J F and Whyte K
633 P 2020 Climate change effects on biodiversity, ecosystems, ecosystem services,
634 and natural resource management in the United States *Science of The Total*
635 *Environment* **733** 137782

636 Whelan M E, Lennartz S T, Gimeno T E, Wehr R, Wohlfahrt G, Wang Y, Kooijmans L M
637 J, Hilton T W, Belviso S, Peylin P, Commane R, Sun W, Chen H, Kuai L,
638 Mammarella I, Maseyk K, Berkelhammer M, Li K-F, Yakir D, Zumkehr A, Katayama
639 Y, Ogée J, Spielmann F M, Kitz F, Rastogi B, Kesselmeier J, Marshall J, Erkkilä K-
640 M, Wingate L, Meredith L K, He W, Bunk R, Launois T, Vesala T, Schmidt J A,
641 Fichot C G, Seibt U, Saleska S, Saltzman E S, Montzka S A, Berry J A and
642 Campbell J E 2018 Reviews and syntheses: Carbonyl sulfide as a multi-scale
643 tracer for carbon and water cycles *Biogeosciences* **15** 3625–57 Online:
644 <https://bg.copernicus.org/articles/15/3625/2018/>

- 645 Wibrál M, Priesemann V, Kay J W, Lizier J T and Phillips W A 2017 Partial information
646 decomposition as a unified approach to the specification of neural goal functions
647 *Brain Cogn* **112** 25–38 Online:
648 <https://linkinghub.elsevier.com/retrieve/pii/S027826261530021X>
- 649 Williams M, Richardson A D, Reichstein M, Stoy P C, Peylin P, Verbeeck H, Carvalhais
650 N, Jung M, Hollinger D Y, Kattge J, Leuning R, Luo Y, Tomelleri E, Trudinger C M
651 and Wang Y-P 2009 Improving land surface models with FLUXNET data
652 *Biogeosciences* **6** 1341–59 Online: <https://bg.copernicus.org/articles/6/1341/2009/>
- 653 Williams P L and Beer R D 2010 Nonnegative Decomposition of Multivariate Information
654 Online: <http://arxiv.org/abs/1004.2515>
- 655 Wood D A 2021 Net ecosystem carbon exchange prediction and insightful data mining
656 with an optimized data-matching algorithm *Ecol Indic* **124** 107426 Online:
657 <https://linkinghub.elsevier.com/retrieve/pii/S1470160X21000911>
- 658 Wutzler T, Lucas-Moffat A, Migliavacca M, Knauer J, Sickel K, Šigut L, Menzer O and
659 Reichstein M 2018 Basic and extensible post-processing of eddy covariance flux
660 data with REddyProc *Biogeosciences* **15** 5015–30 Online:
661 <https://bg.copernicus.org/articles/15/5015/2018/>
- 662 Xiao W, Wei Z and Wen X 2018 Evapotranspiration partitioning at the ecosystem scale
663 using the stable isotope method—A review *Agric For Meteorol* **263** 346–61 Online:
664 <https://linkinghub.elsevier.com/retrieve/pii/S0168192318303009>
- 665 Yang Y, Cui Y, Bai K, Luo T, Dai J, Wang W and Luo Y 2019 Short-term forecasting of
666 daily reference evapotranspiration using the reduced-set Penman-Monteith model
667 and public weather forecasts *Agric Water Manag* **211** 70–80 Online:
668 <https://linkinghub.elsevier.com/retrieve/pii/S0378377418314732>
- 669 Yetemen O, Istanbuluoglu E, Flores-Cervantes J H, Vivoni E R and Bras R L 2015
670 Ecohydrologic role of solar radiation on landscape evolution *Water Resour Res* **51**
671 1127–57 Online: <http://doi.wiley.com/10.1002/2014WR016169>
- 672 Yusup Y and Liu H 2020 Effects of persistent wind speeds on turbulent fluxes in the
673 water-atmosphere interface *Theor Appl Climatol* **140** 313–25 Online:
674 <http://link.springer.com/10.1007/s00704-019-03084-4>
- 675 Zeng S, Xia J, Chen X, Zou L, Du H and She D 2020 Integrated land-surface
676 hydrological and biogeochemical processes in simulating water, energy and carbon
677 fluxes over two different ecosystems *J Hydrol (Amst)* **582** 124390 Online:
678 <https://linkinghub.elsevier.com/retrieve/pii/S0022169419311254>
- 679 Zhao W L, Qiu G Y, Xiong Y J, Paw U K T, Gentile P and Chen B Y 2020 Uncertainties
680 Caused by Resistances in Evapotranspiration Estimation Using High-Density Eddy
681 Covariance Measurements *J Hydrometeorol* **21** 1349–65 Online:
682 <https://journals.ametsoc.org/view/journals/hydr/21/6/JHM-D-19-0191.1.xml>

683 Zhou S, Yu B, Zhang Y, Huang Y and Wang G 2018 Water use efficiency and
684 evapotranspiration partitioning for three typical ecosystems in the Heihe River
685 Basin, northwestern China *Agric For Meteorol* **253–254** 261–73 Online:
686 <https://linkinghub.elsevier.com/retrieve/pii/S016819231830039X>

687

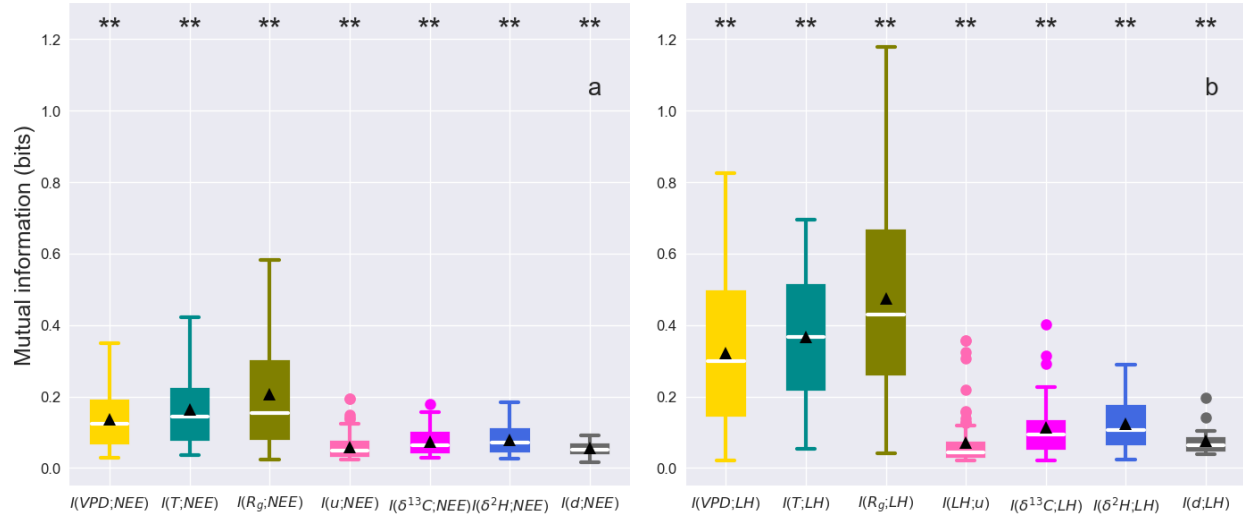


Figure 1 (a) Individual mutual information, $I(X;Y)$, shared between net ecosystem exchange, NEE , and each individual meteorological variable (vapor pressure deficit, VPD , air temperature, T , global radiation, R_g , windspeed, u). (b) Individual information shared between latent heat flux, LH , and each individual meteorological variable. Boxes of mutual information between meteorological variables and flux are consists of the same quantity that is calculated based on different isotope availability (e.g., box of $I(VPD; NEE)$ consists of $I(VPD; NEE)$ based on the availability of $\delta^{13}C$, $I(VPD; NEE)$ based on the availability of δ^2H , and $I(VPD; NEE)$ on the availability of d , collectively). The mean and median values of each boxplot are shown as black triangle and white line, respectively. The double asterisk indicates a significant p-value (<0.01).

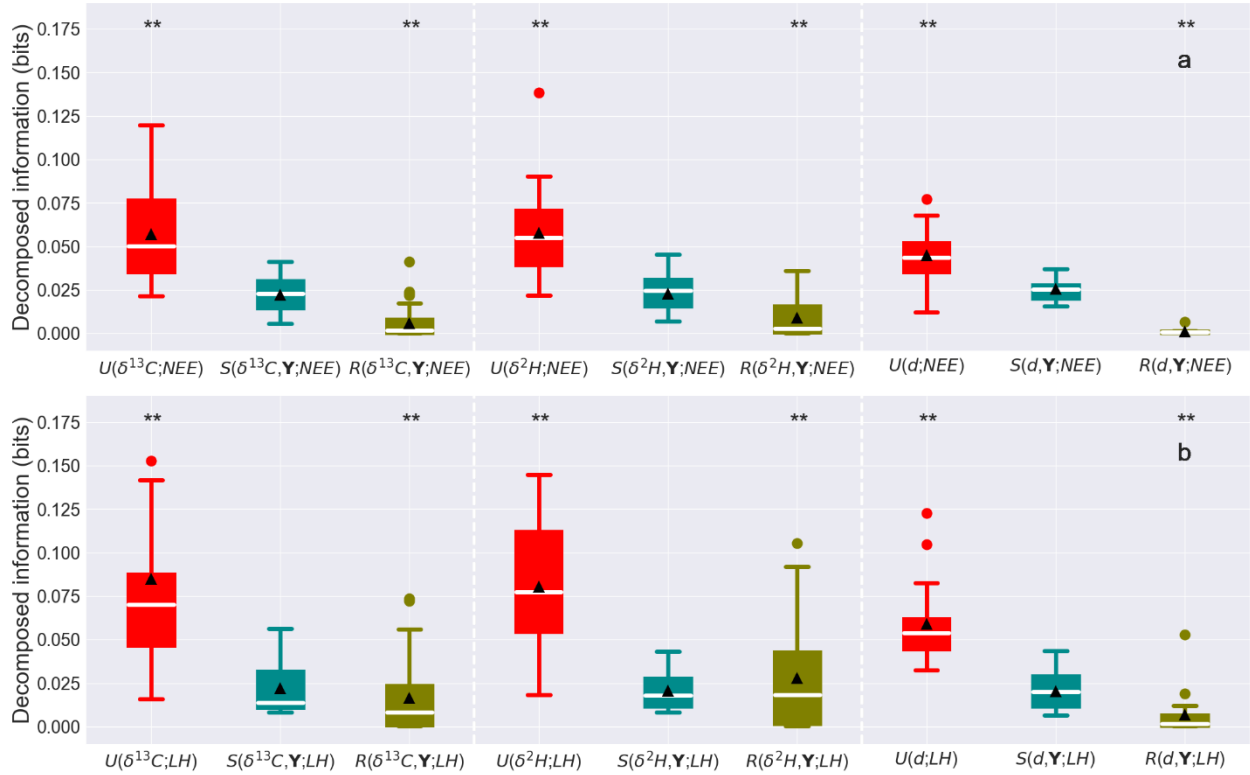


Figure 2 (a) The unique information, U , synergistic information, S , and redundant information, R , of the $\delta^{13}\text{C}$, $\delta^2\text{H}$, and d stable isotope flux ratios on the net ecosystem exchange, NEE , and (b) latent heat flux, LH . The values of S , and R are calculated by averaging across different meteorological variables, indicated by Y (e.g., the average over $S(\delta^2\text{H}, VPD; LH)$, $S(\delta^2\text{H}, T; LH)$, $S(\delta^2\text{H}, u; LH)$, and $S(\delta^2\text{H}, R_g; LH)$ for S). The mean and median values of each boxplot are shown as black triangle and white line, respectively. The double asterisk indicates a significant p-value (<0.01).

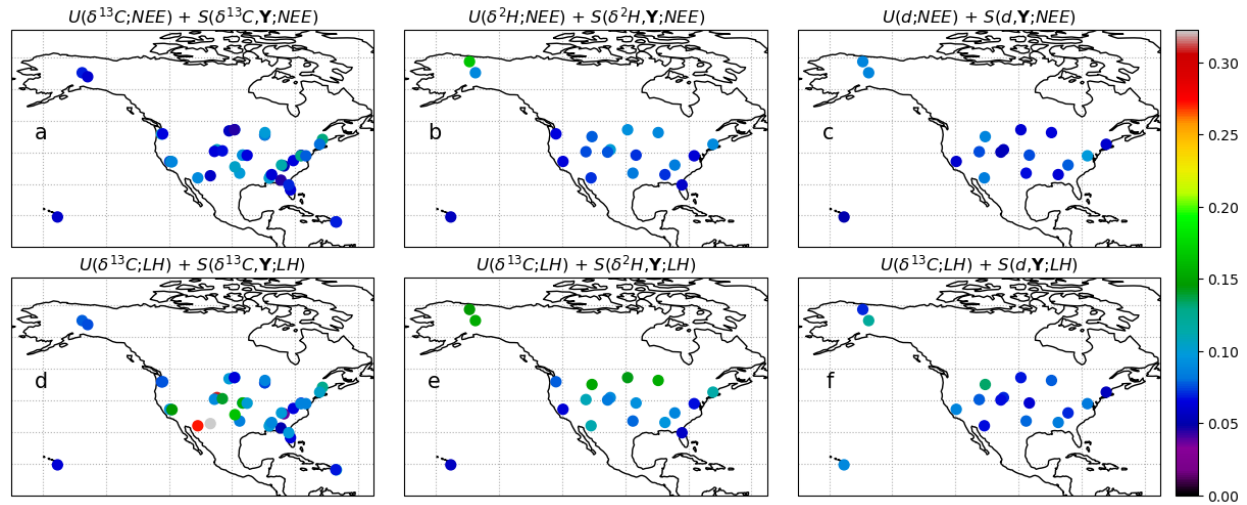


Figure 3 The additive information of (a) $\delta^{13}\text{C}$, (b) $\delta^2\text{H}$, and (c) d isotope data about net ecosystem exchange, NEE . The additive information of (d) $\delta^{13}\text{C}$, (e) $\delta^2\text{H}$, and (f) d isotope data about latent heat flux, LH . The additive information is the sum unique, U , and synergistic, S , information added by each data source.

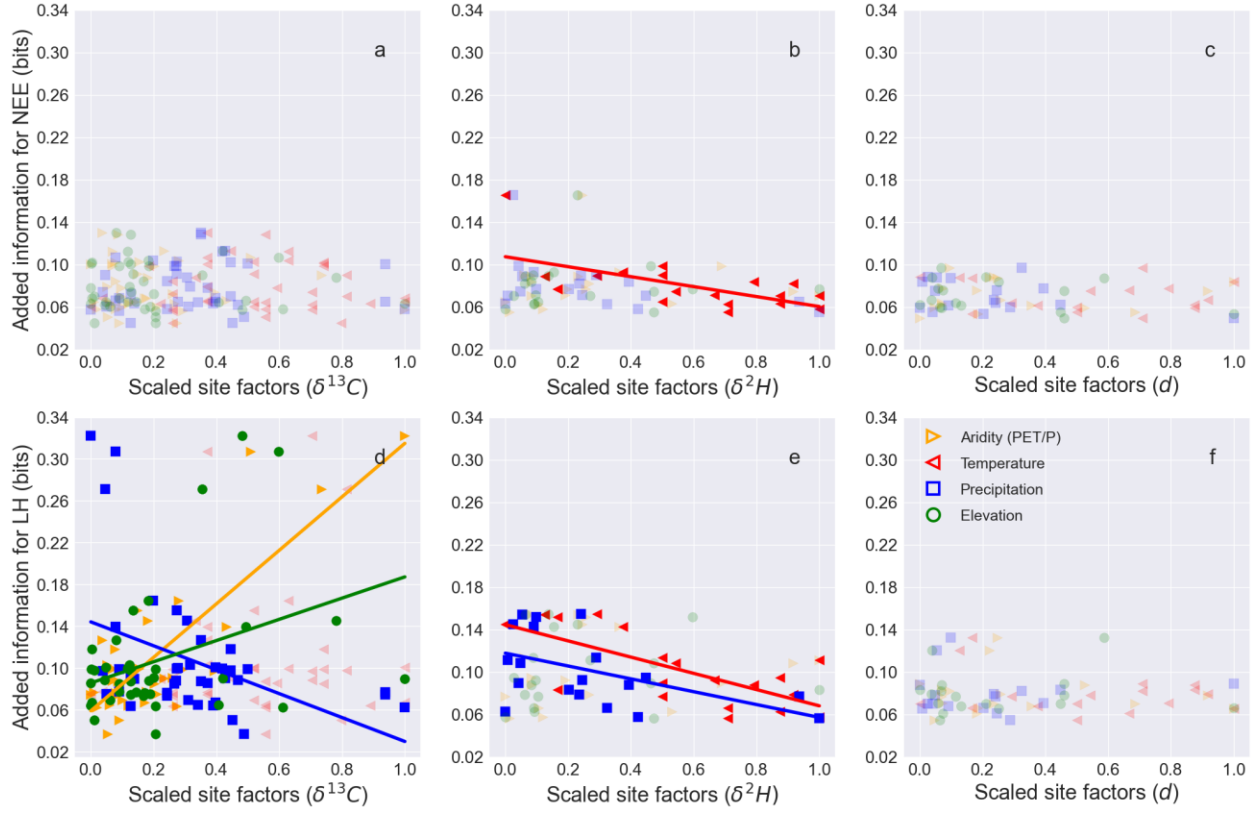


Figure 4 The total added information of (a) $\delta^{13}C$, (b) δ^2H , and (c) d isotope data about net ecosystem exchange, NEE , against scaled site-specific variables. The total added information of (d) $\delta^{13}C$, (e) δ^2H , and (f) d isotope data about latent heat flux, LH against scaled site-specific variables. Solid lines indicate a significant p-values (< 0.05) of the slopes.